Stem Cell Reports, Volume *12*

Supplemental Information

The Dlg Module and Clathrin-Mediated Endocytosis Regulate EGFR Signaling and Cyst Cell-Germline Coordination in the *Drosophila* Testis

Fani Papagiannouli, Cameron Wynn Berry, and Margaret T. Fuller

Supplemental Information

The Dlg-module and clathrin-mediated endocytosis regulate EGFR signaling and cyst cell-germline coordination in the *Drosophila* testis.

Fani Papagiannouli, Cameron Wynn Berry, Margaret T. Fuller

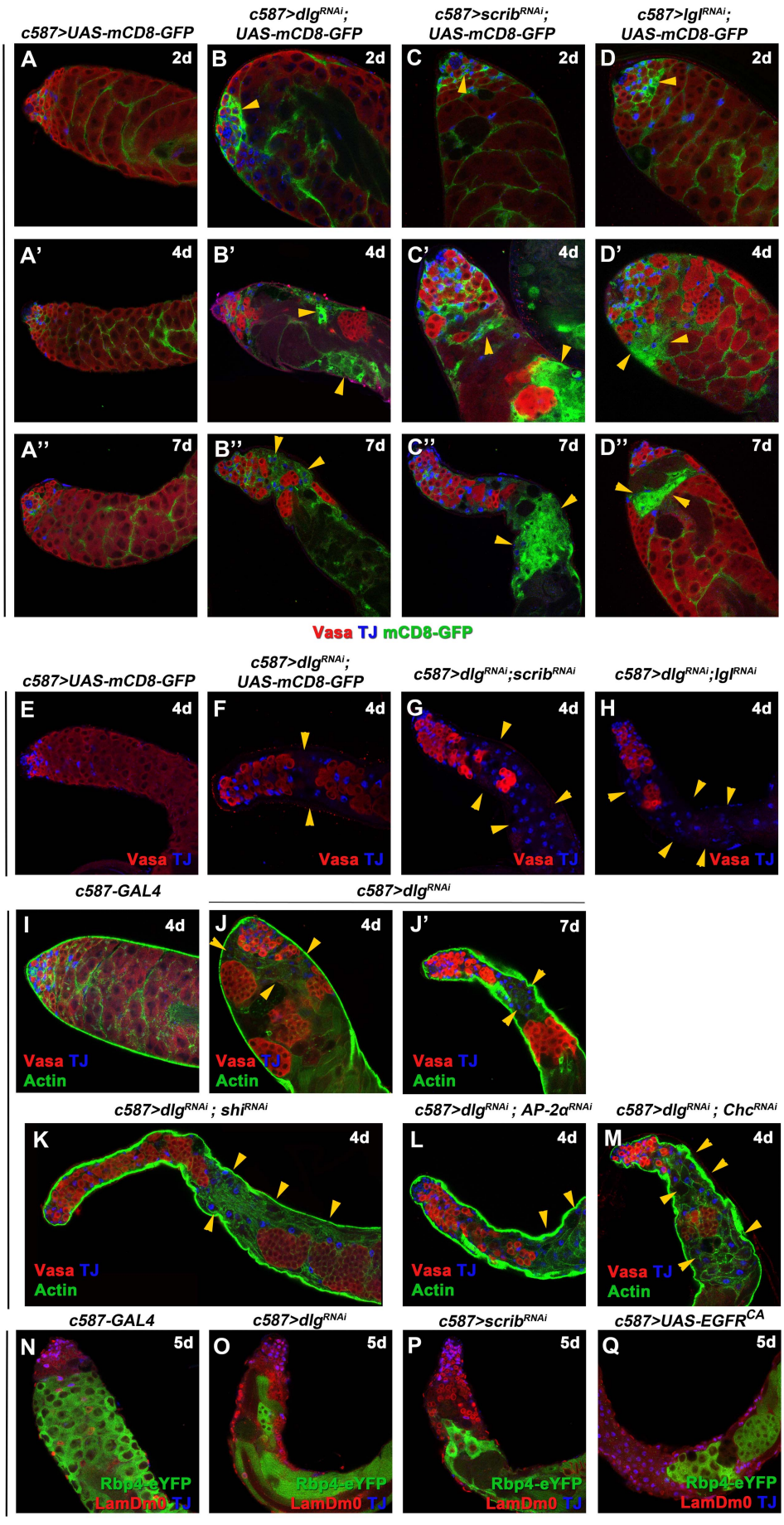
c587>UAS-mCD8-GFP
c587>dlg^RNAi; UAS-mCD8-GFP
c587>scrib^RNAi; UAS-mCD8-GFP
c587>lgl^RNAi; UAS-mCD8-GFP
A 2d
B 2d
C 2d
D 2d
A' 4d
B' 4d
C' 4d
D' 4d
A'' 7d
B'' 7d
C'' 7d
D'' 7d
Vasa TJ mCD8-GFP
c587>UAS-mCD8-GFP
c587>dlg^RNAi; UAS-mCD8-GFP
c587>dlg^RNAi;scrib^RNAi
c587>dlg^RNAi;lgl^RNAi
E 4d
F 4d
G 4d
H 4d
Vasa TJ
c587-GAL4
c587>dlg^RNAi
I 4d
J 4d
J' 7d
Vasa TJ Actin
c587>dlg^RNAi ; shi^RNAi
c587>dlg^RNAi ; AP-2α^RNAi
c587>dlg^RNAi ; Chc^RNAi
K 4d
L 4d
M 4d
c587-GAL4
c587>dlg^RNAi
c587>scrib^RNAi
c587>UAS-EGFR^CA
N 5d
O 5d
P 5d
Q 5d
Rbp4-eYFP LamDm0 TJ

Figure S1: Knockdown *dlg*, *scrib*, *lgl* or clathrin-mediate endocytosis in cyst cells leads to cell non-autonomous germ cell death and comparable defects in double knockdown combinations. Related to Fig. 1 and 4. Adult testes of the indicated genotypes in the background of the *Gal80^{ts}* **(A-D'')** *mCD8-GFP* (green) expressed in cyst cells; anti-Vasa (red; germline); anti-TJ (blue; early cyst cell nuclei). Yellow arrowheads: mCD8-positive cyst cell regions. **(E-H)** immunostainings with anti-Vasa (red) and anti-TJ (blue). **(I-M)** immunostainings with anti-Vasa (red; germline), anti-TJ (blue; early cyst cell nuclei) and F-actin stained for phalloidin (green; cyst cells and germline fusome). **(N-Q)** immunostainings with anti-LamDm0 (red), anti-TJ (blue) and anti-GFP (green) for Rbp4-positive spermatocytes. Yellow arrowheads indicate cyst cell clusters. Newly eclosed male flies were shifted at 30^{o}C to activate the RNAi for 2, 4 and 7 days (d). Testes oriented with anterior at left. Image frame 246µm.

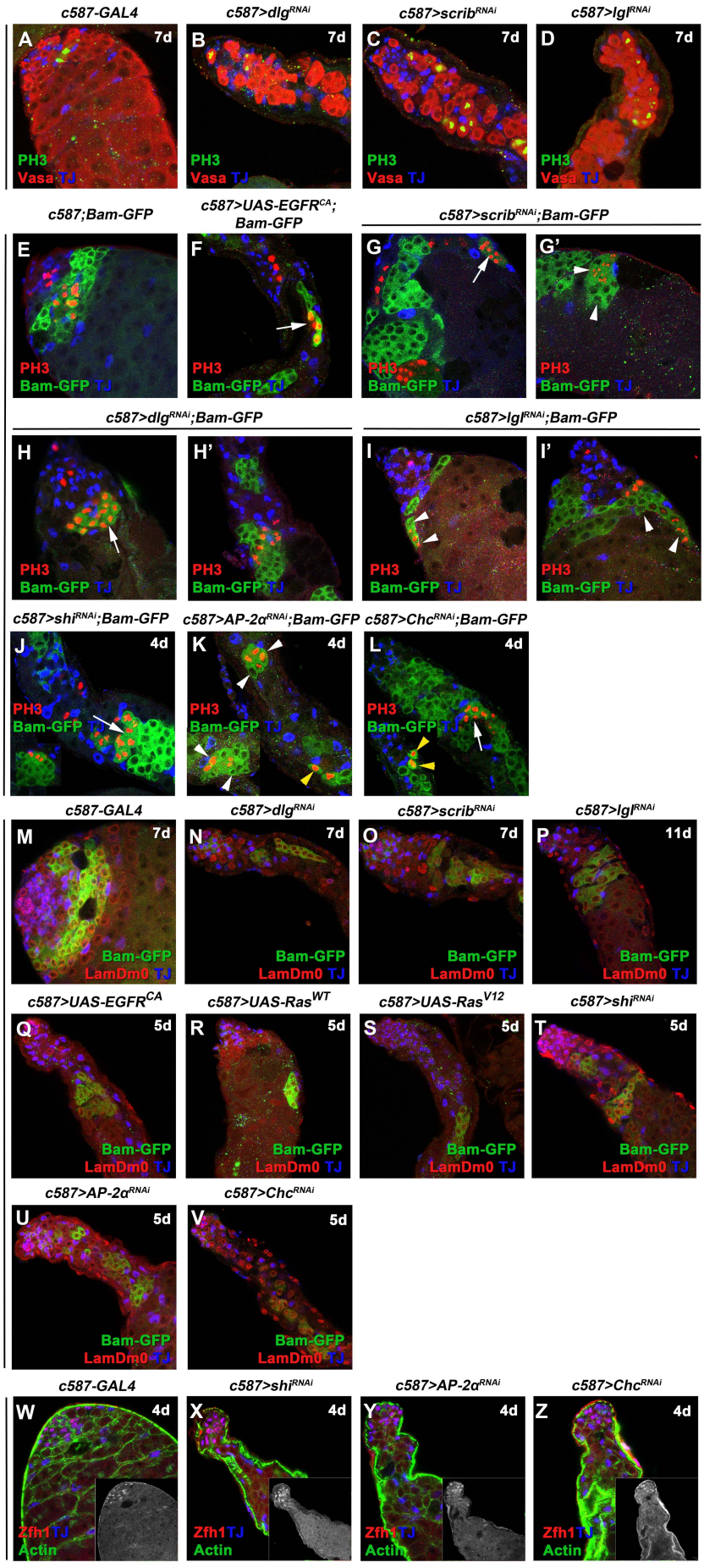
c587-GAL4
c587>dlg^RNAi
c587>scrib^RNAi
c587>lgl^RNAi
A 7d
B 7d
C 7d
D 7d
PH3
Vasa TJ
c587;Bam-GFP
c587>UAS-EGFR^CA; Bam-GFP
c587>scrib^RNAi;Bam-GFP
E
F
G
G'
PH3
Bam-GFP TJ
c587>dlg^RNAi;Bam-GFP
c587>lgl^RNAi;Bam-GFP
H
H'
I
I'
c587>shi^RNAi;Bam-GFP
c587>AP-2α^RNAi;Bam-GFP
c587>Chc^RNAi;Bam-GFP
J 4d
K 4d
L 4d
c587-GAL4
c587>dlg^RNAi
c587>scrib^RNAi
c587>lgl^RNAi
M 7d
N 7d
O 7d
P 11d
Bam-GFP
LamDm0 TJ
c587>UAS-EGFR^CA
c587>UAS-Ras^WT
c587>UAS-Ras^V12
c587>shi^RNAi
Q 5d
R 5d
S 5d
T 5d
c587>AP-2α^RNAi
c587>Chc^RNAi
U 5d
V 5d
c587-GAL4
c587>shi^RNAi
c587>AP-2α^RNAi
c587>Chc^RNAi
W 4d
X 4d
Y 4d
Z 4d
Zfh1 TJ
Actin

Figure S2: Knockdown of *dlg, scrib, lgl* and CME components or EGFR overactivation in cyst cells results in similar non-autonomous loss of spermatogonia and spermatocytes, while remaining germ cells retain their proliferation capacity. **Related to Fig. 1, 2 and 4**. Adult testes of the indicated genotypes in the background of the *Gal80^{ts}*. **(A-D)** immunostainings with anti-Vasa (red; germline), anti-TJ (blue; early cyst cell nuclei) and anti-PH3 (green) marking cells in mitosis. **(E-L)** Bam-GFP transgene (red) expressed in late spermatogonia, anti-TJ (blue; early cyst cell nuclei) and anti-PH3 (green) marking cells in mitosis. Arrows point at Bam-positive spermatogonial cysts that divide synchronously. White arrowheads point at Bam-positive spermatogonial cysts that divide asynchronously as not all germ cells within each cyst are PH3 positive. Yellow arrowheads point at Bam-positive spermatogonia. **(M-V)** Bam-GFP transgene (green) in late spermatogonia, anti-LamDm0 (red) marking cyst cells and early germ cells (GSCs, GBs and spermatogonia), anti-TJ (blue; early cyst cell nuclei). (A'-J') higher magnifications of testes apical region. **(W-Z)** immunostainings with anti-Zfh1 (red; CySCs and daughters), anti-TJ (blue) and Phalloidin (green; F-actin). Small inset pictures show the Zfh-1 panels from (W-Z). Testes oriented with anterior at left. Image frame (A-V) 123μm, (W-Z) 246μm.

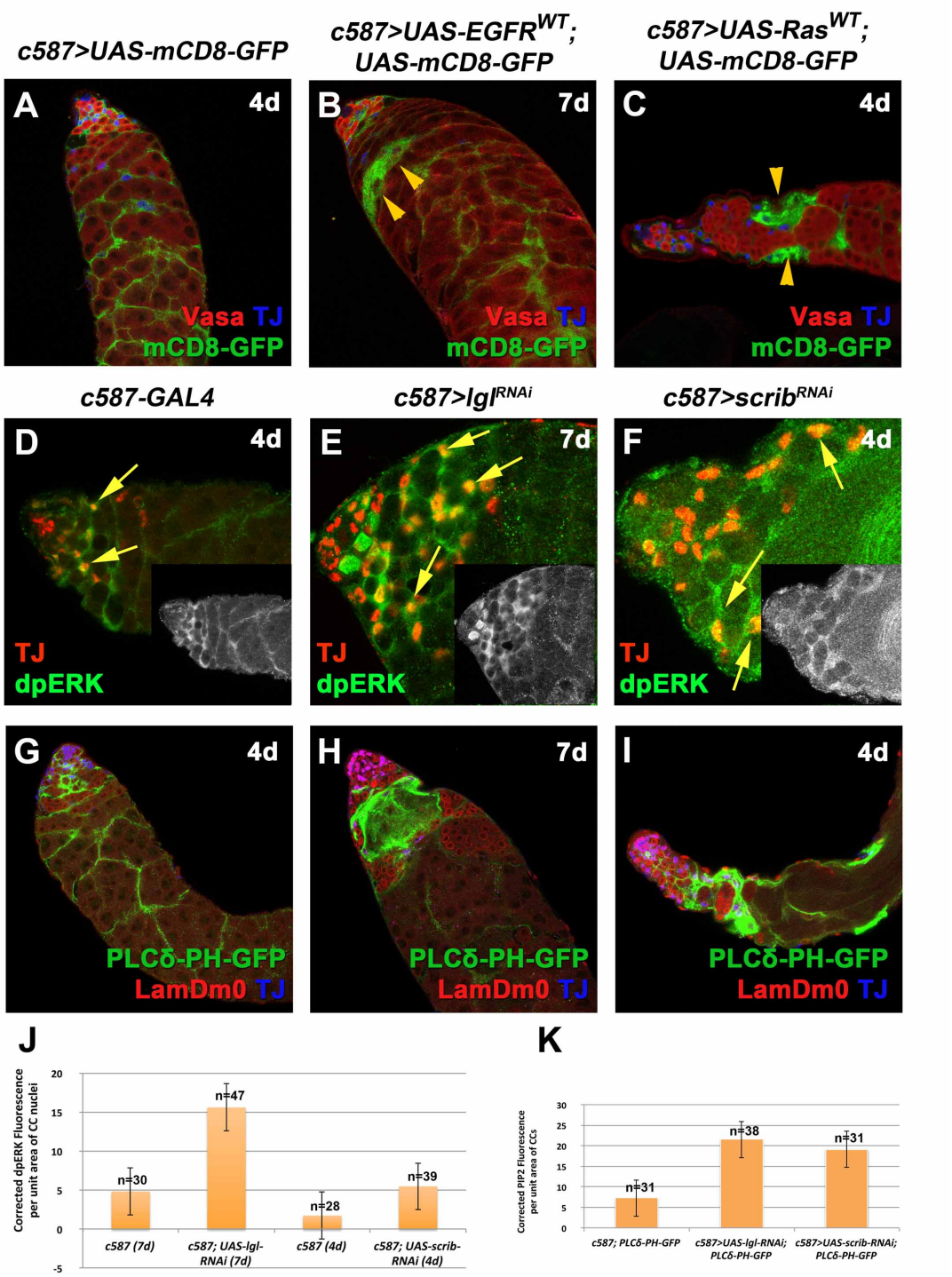

Figure S3: Knockdown of *scrib* and *lgl* or overactivation of EGFR receptor signaling in cyst cells have similar phenotypes. Related to Fig. 2. (A-C) *mCD8-GFP* (green) expressed in cyst cells; anti-Vasa (red; germline) and anti-TJ (blue; early cyst cell nuclei). **(D-F)** anti-TJ (red) and anti-dpERK (green). Yellow arrows: examples of cyst cells double-labeled for TJ and dpERK. Small inset pictures show the anti-dpERK staining only. **(G-I)** the PIP2 reporter PLCδ-PH-GFP expressed in cyst cells (green), anti-LamDm0 (red) marking cyst cells and early germ cells (GSCs, GBs and spermatogonia), anti-TJ (blue; early cyst cell nuclei). **(J)** Quantification of corrected fluorescent dpERK levels in cyst cell (CC) nuclei depleted of *scrib* and *lgl* function. **(K)** Quantification of corrected fluorescent PIP2 levels in cyst cells (CC) via the PLCδ-PH-GFP reporter. Testes oriented with anterior at left. Image frame (A-C, G-I) 246µm, (D-F) 123µm.

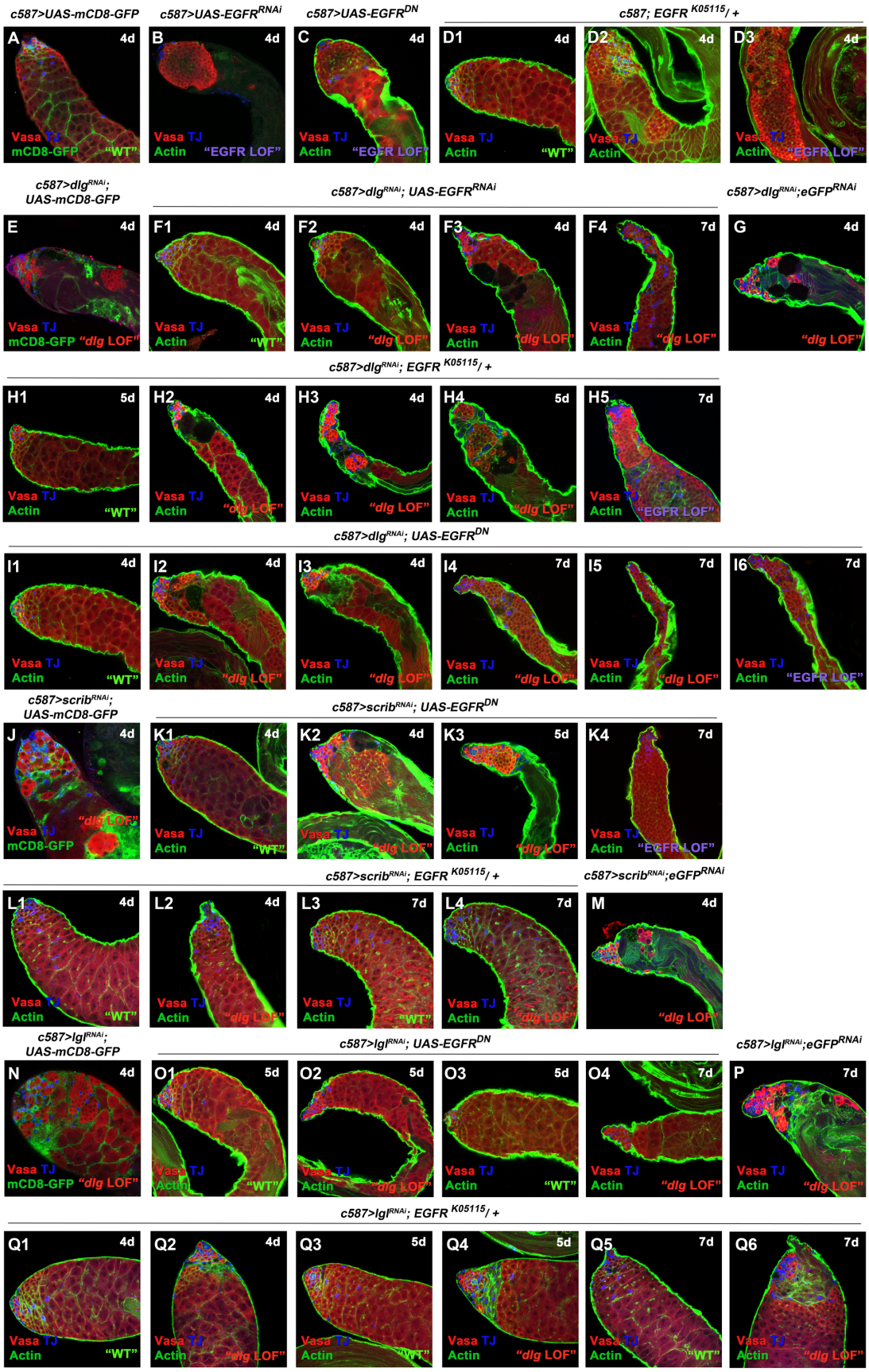

Figure S4: Lowering EGFR signaling levels can rescue the *dlg*, *scrib* and *lgl* loss of function phenotypes in adult testis. Related to Fig. 3. Adult testes of the indicated genotypes in the background of the *Gal80^{ts}*. Testes immunostained with anti-Vasa (red; germline), anti-TJ (blue; early cyst cell nuclei) and either anti-GFP (green) for the *mCD8-GFP* expressed in cyst cells or Phalloidin

(green; F-actin in cyst cells and germline fusome) depending on the genotype. Representative pictures for each genotype used, and the phenotypic classes accompanying them are shown. Order of phenotypic strength: weak and strong "dlg LOF", "wt" and "EGFR LOF". Newly eclosed male flies were shifted at 30^{o}C to activate the RNAi for 4, 5 and 7 days. Testes oriented with anterior at left. Image frame 246μm.

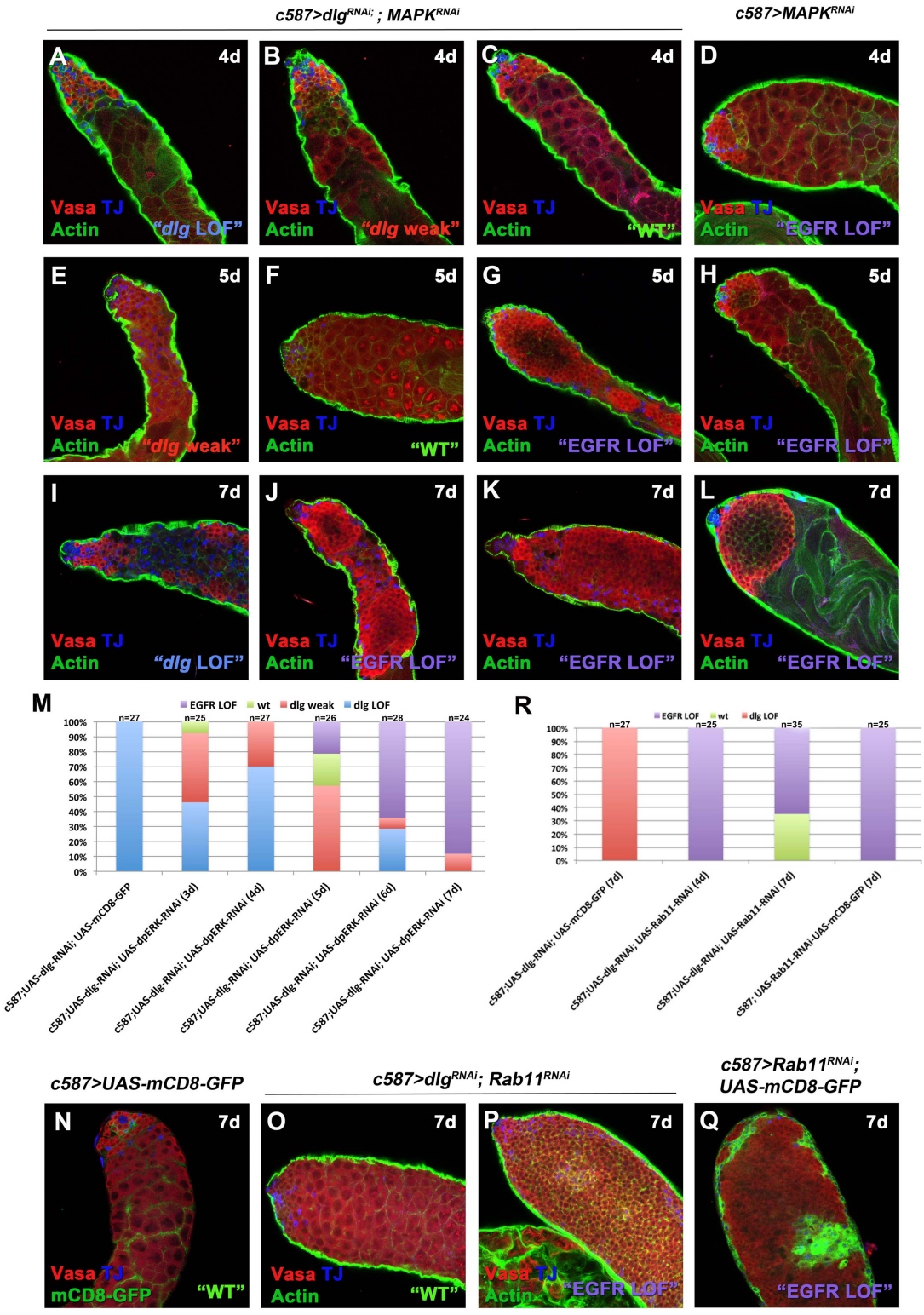

Figure S5: Lowering EGFR signaling levels by knocking down the MAPK or recycling endosome component Rab11 in cyst cells can rescue the *dlg* defects in cyst cells. Related to Fig. 3 and 5. Adult testes of the indicated genotypes in the background of the *Gal80*^{ts}. Newly eclosed male flies were shifted at 30^{o}C to activate the RNAi for 4, 5 and 7 days. **(A-M) Knockdown of MAPK in cyst cells. (A-L)** F-actin stained for phalloidin (green; cyst cells and germline fusome); anti-Vasa (red); anti-TJ (blue). Double-knockdown of MAPK and *dlg* by RNAi in cyst cells for 3-5 days resulted in partially rescued weak *dlg* phenotypes (Fig.S6B, S6E) or even resembled the wild type controls (Fig.S6C). In double-knockdowns for 6-7 days, less than 30% of the testes scored showed the "dlg LOF" phenotype and the majority of testes fell in the "EGFR LOF" class (Fig. S6K, S6M). **(M)** Quantifications of the

different phenotypic classes accompanying each genotype, organized in order of phenotypic strength: “dlg LOF”, “dlg weak”, “wt” and “EGFR LOF”. **(N-R) Knockdown of Rab11 in cyst cells. (N, Q)** *mCD8-GFP* (green) expressed in cyst cells; anti-Vasa (red; germline); anti-TJ (blue; early cyst cell nuclei), **(O, P)** F-actin stained for phalloidin (green; cyst cells and germline fusome); anti-Vasa (red); anti-TJ (blue). **(R)** Quantifications of the different phenotypic classes accompanying each genotype, organized in order of phenotypic strength: “dlg LOF”, “wt” and “EGFR LOF”. Testes oriented with anterior at left. Image frame 246μm.

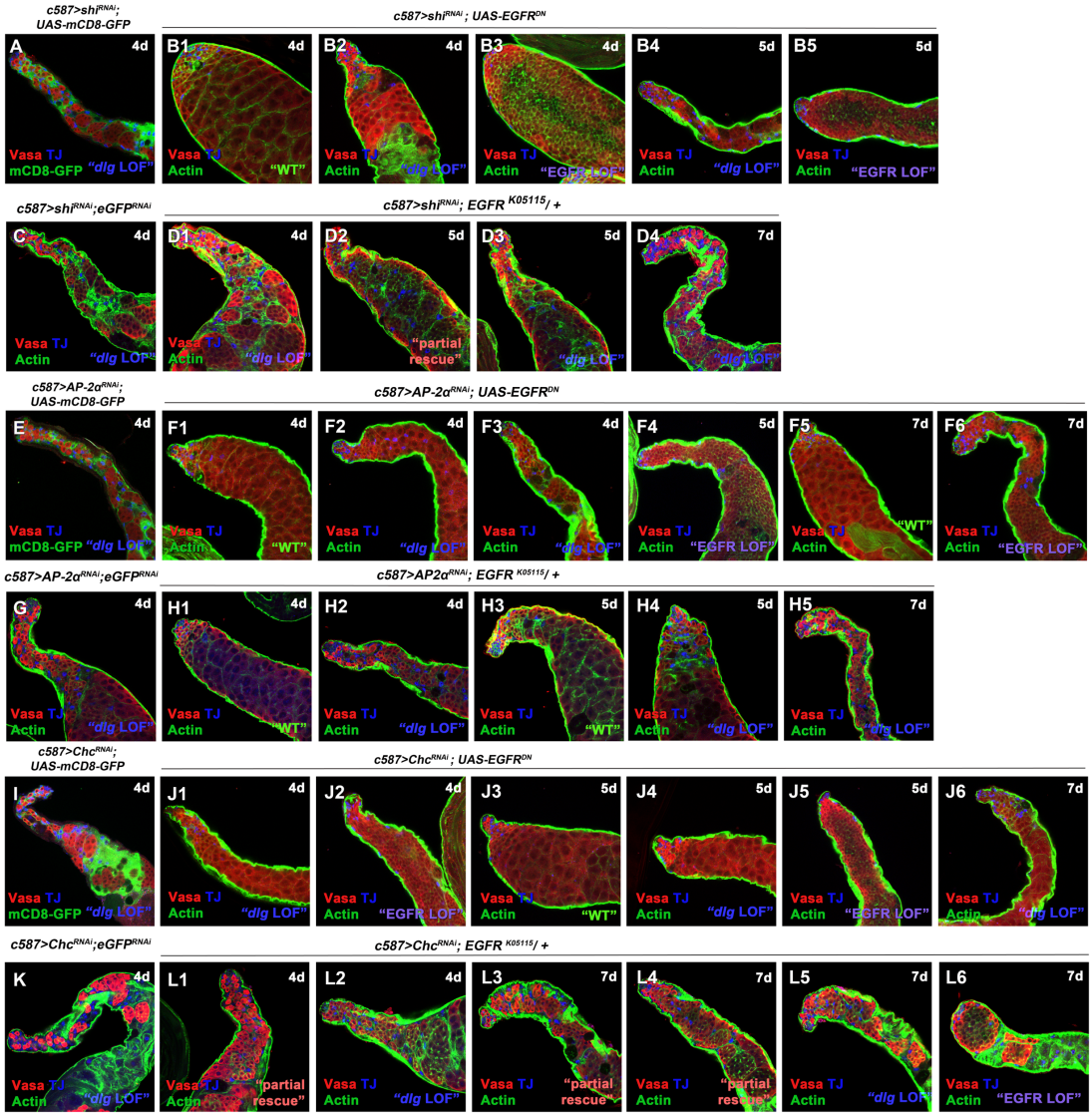

Figure S6: Lowering EGFR signaling levels can rescue the *shi, AP-2α* or *Chc* knockdown phenotypes in cyst cells. **Related to Fig. 5.** Adult testes of the indicated genotypes in the background of the *Gal80^{ts}* immunostained with anti-Vasa (red; germline), anti-TJ (blue; early cyst cell nuclei) and either anti-GFP (green) for the *mCD8-GFP* or Phalloidin (green; F-actin marking cyst cells and germline fusome), depending on the genotype. Representative pictures for each genotype used and the phenotypic classes accompanying them are shown. Order of phenotypic strength: "dlg LOF", "partial rescue", "wt" and "EGFR LOF". Newly eclosed male flies were shifted at 30^{o}C to activate the RNAi for 4, 5 and 7 days. Testes oriented with anterior at left. Image frame 246μm.

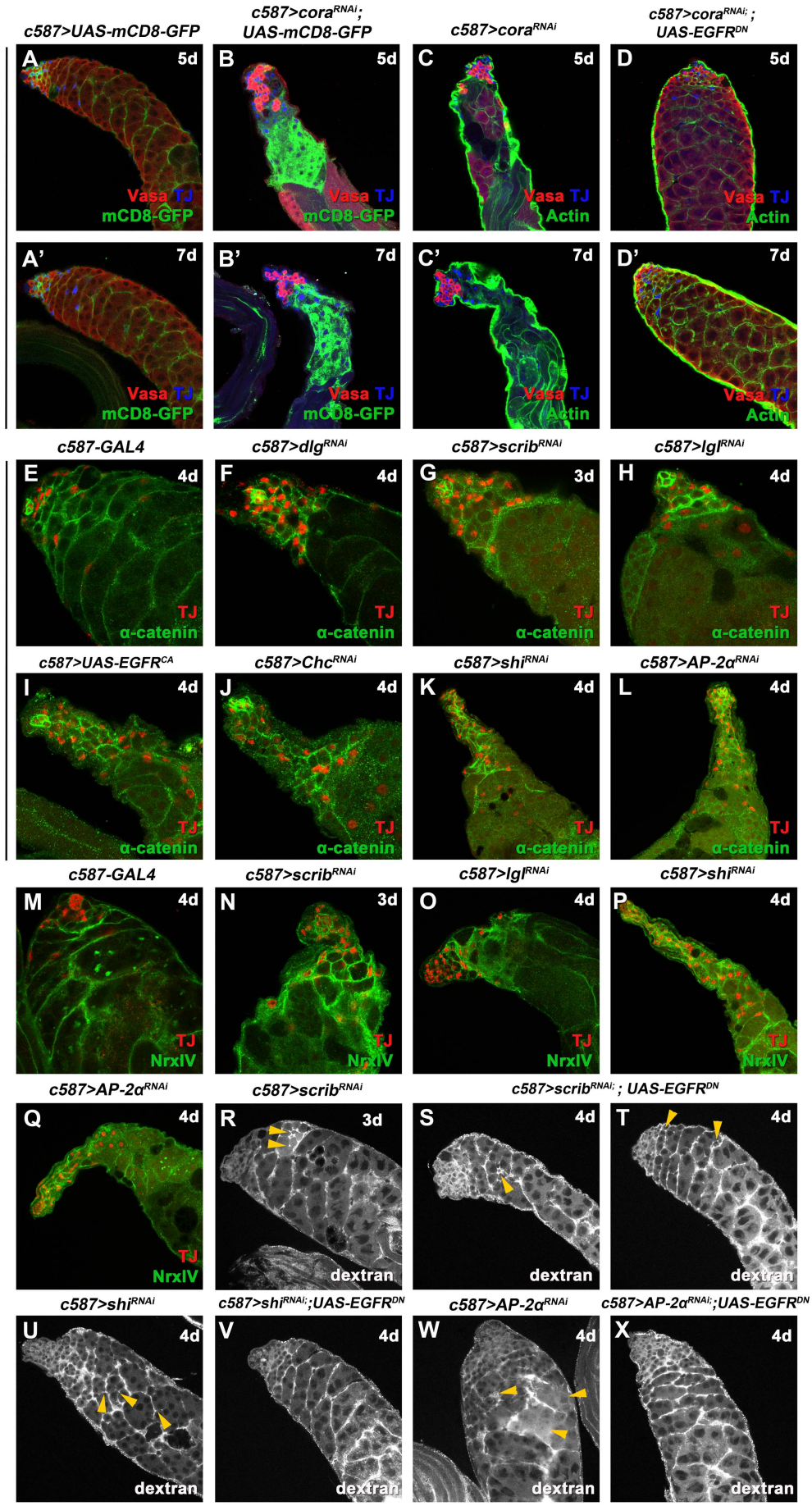
c587>UAS-mCD8-GFP
c587>cora^RNAi; UAS-mCD8-GFP
c587>cora^RNAi
c587>cora^RNAi; UAS-EGFR^DN
A 5d Vasa TJ mCD8-GFP
B 5d Vasa TJ mCD8-GFP
C 5d Vasa TJ Actin
D 5d Vasa TJ Actin
A' 7d Vasa TJ mCD8-GFP
B' 7d Vasa TJ mCD8-GFP
C' 7d Vasa TJ Actin
D' 7d Vasa TJ Actin
c587-GAL4
c587>dlg^RNAi
c587>scrib^RNAi
c587>lgl^RNAi
E 4d TJ α-catenin
F 4d TJ α-catenin
G 3d TJ α-catenin
H 4d TJ α-catenin
c587>UAS-EGFR^CA
c587>Chc^RNAi
c587>shi^RNAi
c587>AP-2α^RNAi
I 4d TJ α-catenin
J 4d TJ α-catenin
K 4d TJ α-catenin
L 4d TJ α-catenin
c587-GAL4
c587>scrib^RNAi
c587>lgl^RNAi
c587>shi^RNAi
M 4d TJ NrxIV
N 3d TJ NrxIV
O 4d TJ NrxIV
P 4d TJ NrxIV
c587>AP-2α^RNAi
c587>scrib^RNAi
c587>scrib^RNAi; UAS-EGFR^DN
Q 4d TJ NrxIV
R 3d dextran
S 4d dextran
T 4d dextran
c587>shi^RNAi
c587>shi^RNAi;UAS-EGFR^DN
c587>AP-2α^RNAi
c587>AP-2α^RNAi;UAS-EGFR^DN
U 4d dextran
V 4d dextran
W 4d dextran
X 4d dextran

Figure S7: Septate junction components share common and distinct characteristics to the Dlg-module and CME components. **Related to Fig. 7.** Adult testes of the indicated genotypes in the background of the *Gal80^{ts}*: **(A-D')** immunostained with anti-Vasa (red; germline), anti-TJ (blue; early cyst cell nuclei) and either anti-GFP (green) for the *mCD8-GFP* or Phalloidin (green; F-actin marking cyst cells and germline fusome), depending on the genotype, **(E-L)** stained with anti-TJ (red) and anti-GFP (green) for the endogenous α-Catenin-YFP, **(M-Q)** stained with anti-TJ (red) and anti-GFP (green) for the endogenous NrxIV-GFP, **(R-X)** dextran dye stained with streptavidin, showing that the dye can access late spermatogonia and spermatocytes when the permeability of testis barrier is compromised or defective. Yellow arrowheads point at examples of permeability defects. Newly eclosed male flies were shifted at 30^{o}C to activate the RNAi for 4, 5 and 7 days, as indicated. Testes oriented with anterior at left. Image frame (A-D', R-X) 246μm, (E-Q) 123μm.

SUPPLEMENTAL EXPERIMENTAL PROCEDURES

Fly stocks and husbandry

The following stocks were obtained from the Bloomington Stock Center (BL) Indiana: *UAS-sktl-RNAi$^{TRiP.JF02796}$*, *UAS-sktl-RNAi$^{TRiP.GL00072}$*, *UAS-ERK-RNAi$^{TRiP.HMS00173}$*, *UAS-scrib-RNAi$^{TRiP.HMS01490}$*, *UAS-AP2α (adaptin)-RNAi$^{TRiP.HMS00653}$*, *UAS-shi-RNAi$^{TRiP.JF03133}$*, *UAS-EGFR-RNAi$^{TRiP.HMS05003}$*, *UAS-sktl-RNAi$^{TRiP.JF02796}$* (BL27715), *UAS-sktl-RNAi$^{TRiP.GL00072}$* (BL35198), *UAS-EGFR^{DN}* (BL5364), *UAS-EGFR^{CA}* (BL9533), *UAS-EGFR^{WT}* (BL5368), *UAS-shi^{ts1}* (BL44222), *UAS-Ras85D^{V12}* (BL4847), *UAS-mCD8-GFP* (BL5139), *Pin/CyO; UAS-mCD8-GFP* (BL5130), *PLCδ-PH-GFP* (BL57353), *P{lacW}EGFR^{K05115}/CyO* (BL10385), *αtub84B-GAL80^{ts}/TM2* (BL7017), *tub-GAL80^{ts}; TM2/TM6B,Tb* (BL7019), *lgl-GAL4^{GMR27F03}* (BL47341) (Papagiannouli, 2013). The following stocks used in this study were obtained from the Vienna *Drosophila* RNAi Center (VDRC) Austria: *UAS-dlg-RNAi^{v41134}, UAS-dlg-RNAi^{v41136}/TM3, UAS-lgl-RNAi^{v109604}, UAS-lgl-RNAi^{v51247}, UAS-Chc-RNAi^{v103383} , UAS-Chc-RNAi^{v32666} , UAS-EGFR-RNAi^{v43267} , UAS-Ras85D-RNAi^{v28129} UAS-Rab11-RNAi^{v22198}, UAS-Rab11-RNAi^{v108382}, UAS-cora-RNAi^{v9787}*. The *scrib-GFP^{CA07683}* and *NrxIV-GFP^{CA06597}* were obtained from Spradling [GFP project; (Buszczak et al., 2007; Papagiannouli, 2013)], *UAS-Ras85D^{wt}* from B.M. Mechler, Bam-GFP from Dennis McKearin, Rbp4-eGFP (Baker et al., 2015), α-Cat-YFP (CPTI-002510/DGRC115551) from the Kyoto Stock Center, *c587*-GAL4 (S. Hou, National Cancer Institute), *UAS-sktl-GFP* from Antoine Guichet (Gervais et al., 2008). Other fly stocks used in this study are described in FlyBase (www.flybase.org). All *UAS-gene^{RNAi}* stocks are referred to in the text as *gene^{RNAi}* for simplicity reasons. Knockdowns were performed using the *UAS-GAL4* system (Brand and Perrimon, 1993) by combining the *UAS-RNAi* fly lines with the cell-type specific *c587-GAL4* driver (Kai and Spradling, 2004) and *αtub-Gal80^{ts}* (Lee and Luo, 1999).

For the phenotypic analysis in adult *Drosophila* testes: *c587*-GAL4; *αtub-Gal80^{ts}; UAS-mCD8-GFP* or *c587*-GAL4*; αtub-Gal80^{ts}* flies were crossed to *UAS-gene^{RNAi}* flies. Crosses were raised at 18^{o}C until adult flies hatched. Then males with the correct genotype (along with few females) were shifted at 30^{o}C for 2-7 days depending on the experimental needs and the phenotypes were analyzed.

Immunofluorescence staining and microscopy

For whole mount testes immunostaining, testes were dissected in PBS, fixed for 20min in 8% formaldehyde and rinsed twice in 1% PBX (1% Triton-100x in PBS). Testes were permeabilized for 15 min in 1x PBS with 0.6% (vol/vol) Triton-100x and 0.6% (wt/vol) sodium deoxycholate at room temperature, washed twice with PBX and then blocked in 5% Bovine Serum Albumin in 1% PBX for 1h. Testes were incubated with primary antibodies over-night at 4^{o}C and the following day with the secondary antibodies for 2h at room temperature in the dark (Papagiannouli et al., 2014). For testes immunostaining in the presence of GFP, 1% PBT (1% Tween-20 in PBS) was used instead of 1% PBX in all steps. For the TUNEL assay, tissue was processed as described above except that after permeabilization, protocol from In Situ Cell Death Detection Kit (TMR Red, Sigma/Roche) was followed. For the dpERK staining testes were dissected in PBS including the phosphatase inhibitor cocktail 2 (1/100, Sigma P5726), were fixed in 4% formaldehyde including phosphatase inhibitor cocktail 2 (1/100) and all subsequent steps as described above. Testes were mounted in ProLong® Gold Antifade (Thermo Fischer Scientific).

The monoclonal antibodies used in this study: anti-Vasa (1/10; rat), anti-LamC-LC28.26 (1/10; mouse), anti-LamDm0-ADL101 (1/10; mouse), anti-Dlg (1/100, mouse) were obtained from the Developmental Studies Hybridoma Bank developed under the auspices of the NICHD and maintained by The University of Iowa, Department of Biological Sciences, Iowa City, IA 52242. Polyclonal anti-Vasa-dC13 (goat; 1/20) and mouse anti-pHistone H3 (C-2; 1/200) were from Santa Cruz Biotechnology, chicken anti-GFP (13970; 1/10,000) from Abcam and rabbit anti-Phospho-p44/42 MAPK (Erk1/2) (Thr202/Tyr204 #9101; 1/200) from Cell Signaling. Guinea-pig anti-TJ (1/5000) polyclonal antibody was a gift of Dorothea Godt, rabbit anti-Zfh1 (1/5000) was a gift of Ruth Lehmann. Filamentous (F-actin) was stained with Alexa Fluor phalloidin 546 or 647 (1/300, Thermo Fischer Scientific) and DNA with DAPI (Thermo Fischer Scientific). Following secondary antibodies were used: donkey anti-goat Alexa Fluor-488, donkey anti-mouse Alexa Fluor-546 and Alexa Fluor-647, donkey anti-guinea pig Alexa Fluor-546 and Alexa Fluor-647, donkey anti-rat Alexa Fluor-488, donkey anti-rabbit Alexa Fluor-488 and Alexa Fluor-546 from Thermo Fischer Scientific (1/500) and donkey anti-chicken Alexa Fluor-488 from Jackson ImmunoResearch (1/500).

Confocal images were obtained using a Leica SP8 system (1024x1024px, 184μm image frame) (CSIF Beckman Center, Stanford University School of Medicine; CECAD, University of Cologne). Pictures were finally processed with Adobe Photoshop 7.0. Quantifications were done using FiJi/ImageJ by measuring "Corrected Total Cell Fluorescence" (CTCF) [CTCF = Integrated Density - (Area of elected cell X Mean fluorescence of background readings)].

Dextran dye & permeability assays.
A dextran dye (3000MW) -biotin conjugated and fixable- was used to test the permeability of the testis barrier (Molecular Probes, D7135). Testes were dissected in Schneider 2 (S2) *Drosophila* medium with 8%FBS and then were incubated in dextran diluted in S2+8%PBS at a final concentration of 0.2µg/µl for 40min at 25oC. Testes were fixed in 8%FA for 20min and were subsequently stained with fluorescent streptavidin (Streptavidin, Alexa Fluor™ 546 conjugate; S11225; Thermo Scientific).

SUPPLEMENTAL REFERENCES
Baker, C.C., Gim, B.S., and Fuller, M.T. (2015). Cell type-specific translational repression of Cyclin B during meiosis in males. Development *142*, 3394-3402.
Brand, A.H., and Perrimon, N. (1993). Targeted gene expression as a means of altering cell fates and generating dominant phenotypes. Development *118*, 401-415.
Buszczak, M., Paterno, S., Lighthouse, D., Bachman, J., Planck, J., Owen, S., Skora, A.D., Nystul, T.G., Ohlstein, B., Allen, A.*, et al.* (2007). The carnegie protein trap library: a versatile tool for Drosophila developmental studies. Genetics *175*, 1505-1531.
Gervais, L., Claret, S., Januschke, J., Roth, S., and Guichet, A. (2008). PIP5K-dependent production of PIP2 sustains microtubule organization to establish polarized transport in the Drosophila oocyte. Development *135*, 3829-3838.
Kai, T., and Spradling, A. (2004). Differentiating germ cells can revert into functional stem cells in Drosophila melanogaster ovaries. Nature *428*, 564-569.
Lee, T., and Luo, L. (1999). Mosaic analysis with a repressible cell marker for studies of gene function in neuronal morphogenesis. Neuron *22*, 451-461.
Papagiannouli, F. (2013). The internal structure of embryonic gonads and testis development in Drosophila melanogaster requires scrib, lgl and dlg activity in the soma. Int J Dev Biol *57*, 25-34.
Papagiannouli, F., Schardt, L., Grajcarek, J., Ha, N., and Lohmann, I. (2014). The hox gene abd-B controls stem cell niche function in the Drosophila testis. Dev Cell *28*, 189-202.